Hindawi Publishing Corporation
Advances in Condensed Matter Physics
Volume 2010, Article ID 912067, 7 pages
doi:10.1155/2010/912067

Research Article

Supercell Band Calculations and Correlation for High-T_C Copper Oxide Superconductors

T. Jarlborg

DPMC, University of Geneva, 24 Quai Ernest-Ansermet, 1211 Geneva 4, Switzerland

Correspondence should be addressed to T. Jarlborg, thomas.jarlborg@unige.ch

Received 24 June 2009; Accepted 12 August 2009

Academic Editor: Igor Mazin

First principle band calculations based on local versions of density functional theory (DFT), together with results from nearly free-electron models, can describe many typical but unusual properties of the high-T_C copper oxides. The methods and a few of the most important results are reviewed. Some additional calculations are presented, and the problems with the commonly used approximate versions of DFT for oxides are discussed with a few ideas for corrections. It is concluded that rather modest corrections to the approximate DFT, without particular assumptions about strong correlation, can push the ground state towards antiferro magnetic (AFM) order. Spin fluctuations interacting with phonons are crucial for the mechanism of superconductivity in this scenario.

1. Introduction

It is often assumed that strong correlation is important for an understanding of the high-T_C problem [1–3]. The failure of the local approximations to the exchange-correlation functional, such as the local (spin) density approximation, LDA, or LSDA [4–7], to produce the antiferro magnetic (AFM) insulating state of many undoped transition metal oxides is generally quoted as the essential reason for discarding DFT calculations for high-T_C copper oxides [3]. DFT is essentially exact, but the approximations to make it practical for use in real applications seem inappropriate for oxides. However, despite this problem, there are several LDA results that fit to the observed high-T_C properties, provided that doping and supercells are considered in order to account for imperfect lattice conditions such as stripes, phonons, or spin waves [8–10]. Here is presented a short review of those DFT results together with a discussion of the correlation problem and an attempt to include further corrections to LSDA. Estimations of couplings λ caused by spin-phonon coupling (SPC) and pure spin fluctuations are also made.

2. Nearly Free-Electron Model

The spin polarized potential from an AFM order (like that of undoped La_2CuO_4) can be generated from $V_{\mathrm{AFM}}(x) = V_0 \exp(-i\vec{Q} \cdot \vec{x})$, where $\vec{Q} = \pi/a_0$ is at the Brillouin Zone (BZ) boundary, so that there is one Cu site with spin up and one with spin down within a distance a_0 (a_0 is the lattice constant). The potential of the other spin has a phase shift of π. The band dispersion from a 1-dimensional (1D) nearly free-electron model (NFE) is obtained from a 2×2 eigenvalue problem, and it has a gap of $2V_0$ at the zone boundary. Suppose now that an additional potential modulation $V_q(x) = V_q \exp(i\vec{q} \cdot \vec{x})$ exists, and that $|\vec{q}| \ll |\vec{Q}|$, so that its periodicity or "wavelength" is much larger than $2a_0$. The product of these two modulations can be written $V(x) = V_q \exp(-i(\vec{Q} - \vec{q}) \cdot \vec{x})$, where the two amplitudes are combined into one coefficient, V_q. Figure 1 shows the real space configurations along the 100-direction. This potential describes AFM modulations in stripes, with magnetic nodes (Cu with zero moment) separated by $a_0 Q/q$. The values of V_q for phonons or spin waves of different lengths are not known from the NFE model, but some values will be fed in from the ab initio Linear Muffin-Tin Orbital (LMTO, [11, 12]) calculations, as will be described here in after. The LMTO calculations are slow for large supercells. The cells need to be large to cover the periodicity of realistic phonon and/or spin-waves, and so far it has been possible to extend the cells in one direction only, usually the CuO bond direction. In contrast, the NFE model is very simple

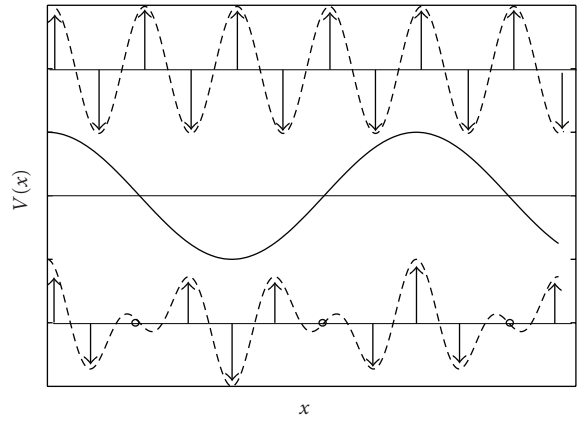

Figure 1: A picture of how stripe-like configurations are made up from the product of two plane wave potentials. The arrows in the upper row show the AFM moments on Cu sites given by the envelope function $\mathrm{Re}(\exp(-i\vec{Q}\cdot\vec{x}))$ (broken line), and the unit cell contains 2 Cu sites along $\vec{x}$. The second row shows the modulation $\mathrm{Re}(\exp(i\vec{q}\cdot\vec{x})$ (here $q = Q/4$) and the last row is the product $\mathrm{Re}(\exp(-i(\vec{Q}-\vec{q})\cdot\vec{x})$ with the new spin configurations on the Cu. The striped unit cell contains 8 Cu sites.

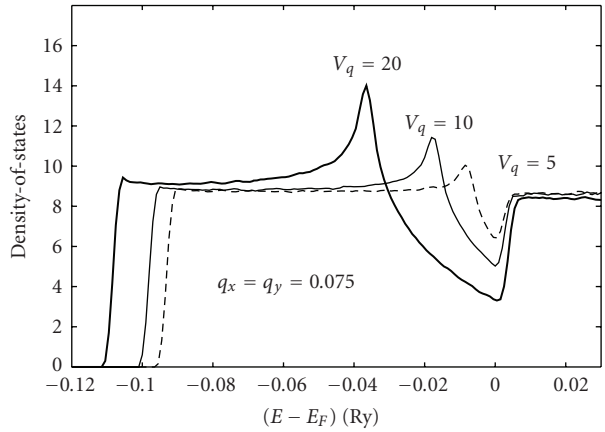

Figure 2: Examples of the DOS from the 2D NFE model for 3 different strengths of V_q (in mRy) for $\vec{q} = (0.075, 0.075)$.

and it can easily be extended to two dimensions (2D). The band dispersion for k-points (k_x, k_y) is now obtained from the eigenvalues of a 3×3 matrix [13]. Not only stripe order but also "checkerboard" configuration can be modeled.

Examples of the density-of-states (DOSs) for 3 different V_q's are shown in Figure 2. The potential modulations are parallel to the CuO bond directions along $\vec{x}$ and $\vec{y}$, and so the gaps appear on the $(k_x, 0)$ and $(0, k_y)$ lines, as shown in Figure 3. However, almost no effect from V_q appears on the band dispersion in the diagonal direction (along (k, k)). Therefore, the Fermi surface (FS) is not affected along the diagonal, but fluctuations, described through amplitude variations of V_q for different positions and different time, will make the FS smeared in the two bond directions. An example of this is shown in Figure 4.

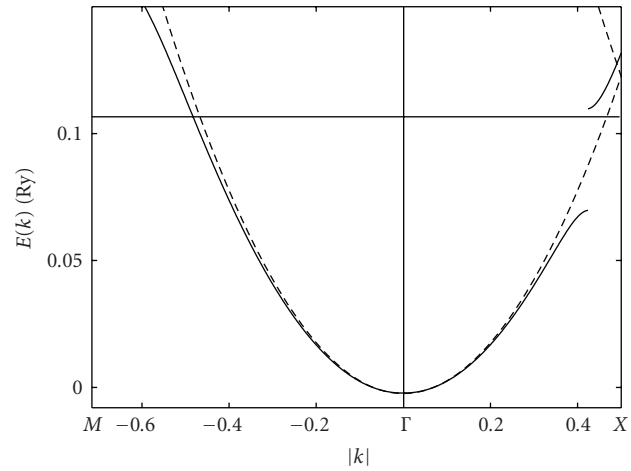

Figure 3: An example of the 2D NFE bands along $(k, 0)$ and (k, k) for $q_x = q_y = 0.075$ and $V_q = 20$ mRy (full line). The FE band without potential perturbations ($V_q = 0$) is shown by the broken line. The thin horizontal line is at the DOS minimum, which is situated at 0.15 holes/cell.

3. Ab Initio 1D-LMTO

By 1D (1-dimensional) LMTO we mean ab initio LMTO calculations for long (and narrow) supercells most often oriented along the CuO bond direction [14, 15]. These calculations are based on the local version of DFT, the local (spin) density approximation, LDA, or LSDA [4, 5]. Cells with phonon distortions and/or spin waves within lengths of 4, 8, and 12 lattice constants are typically considered in these calculations. The wavelengths of spin waves are twice as long as those of phonons. Hole doping, h, in $La_{(2-h)}Ba_hCuO_4$ (LBCO) is generally modeled by the virtual crystal approximation (VCA) where the nuclear and electronic La-charges (57.0) are reduced to $(57-h/2)$ to account for a perfectly delocalized doping (h in holes per Cu). But some calculations with real La/Ba substitutions show that improved superconducting properties can be expected from periodic doping distributions [16]. The maximal phonon distortion, u_i, for different sites, i, and AFM magnetic moments on Cu, m, depend on temperature, T, force constants, and spin stiffness. Appropriate values of $u_i(T)$ and $m(T)$ at $T \approx 100$ K are deduced from experiments and calculations [17–22].

A striking result of these calculations (also made for $HgBa_2CuO_4$) is that a gap (or a pseudogap) will open up in the DOS, very similar to what is found in the NFE models. The gap will appear near to E_F for the undoped material if the wavelengths (Λ) are long, while for short phonons or spin waves the gap moves to lower energy [8]. In summary, $\Lambda = 1/h$, where Λ is in units of a_0 and h is the number of holes per Cu.

A second important result is that the spin waves will be stronger, and the pseudogaps will be deeper, if the waves coexist with phonon distortions of the correct wave length and phase [14]. Interactions between phonons and spin waves have also been suggested in order to explain neutron

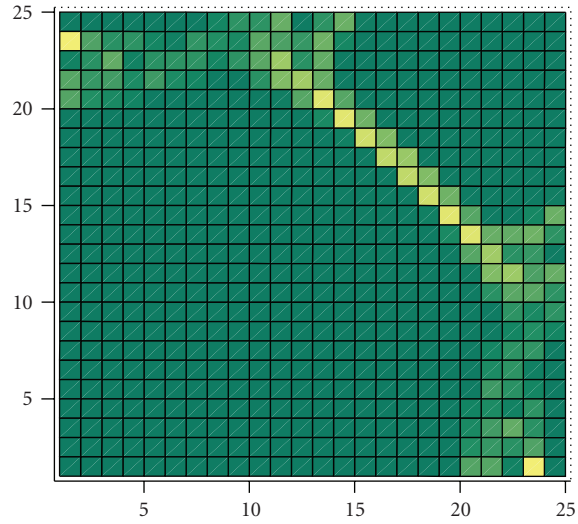

Figure 4: An example of the Fermi surface in the 2D NFE model with fluctuations of V_q. The FS is well defined in the diagonal direction, while the fluctuations makes it diffuse in the x and y-directions.

scattering [23, 24]. Phonons like the "half-breathing" O-mode and modes with z-displacements of La and apical oxygen are most effective in this process of SPC. This mechanism offers direct explanations of phonon softening, q-dependent spin excitations, and various isotope effects [10, 15].

The rather few LMTO results permit to establish only a few values of V_q for different q's, i of the phonons and spin waves. A general trend of larger V_q for long wave lengths seems clear, both for phonons and for spin waves. A procedure based on the partial character of the states above and below the gap in the NFE model confirms this trend for spin waves, and it permits to fill in some of the q-dependent points not calculated by LMTO. In all this gives some confidence in the q, i-variations of V_q. However, one can expect more vivid variations of the spin part near $q \to 0$, because LDA underestimates the transition towards AFM.

When these V_q-values are fed into the 2D NFE model, it gives an approximately linear variation of q as function of h, up to a saturation near $q \sim 0.125$ for h larger than ~ 0.13 [13]. Hence, the linear dependence for low h is in qualitative agreement with the result from 1D-LMTO, but the pace is different. This is probably because the gap opens *both* along x and y in the 2D NFE model, which makes the progression of the gap a bit slower than in 1D. The saturation is because the V_q's decrease for increasing q and it becomes impossible to open a gap at the low energy where E_F should be for large h. However, if q_x and q_y are assumed to be different in the 2D NFE model, it is possible to follow one gap towards lower energy. A second weaker gap moves to higher energy.

4. Superconductivity

The emerging picture from these band results is that moderately strong spin fluctuations, which exist for many combinations of $\vec{q}$ and ω, will be enhanced through SPC to some particular phonon distortions. The selection depends on the atomic character of the phonon mode as well as on doping and wave length (i.e., on $\vec{q}$). The latter is because the pseudogap appears at E_F so that a maximum amount of kinetic energy can be gained from the SPC mode. This is for low T when the states below the gap is of one spin and well separated from the (unoccupied) state of the other spin above the gap. But for increasing T there will be mixed occupations of the states around E_F through the Fermi-Dirac function (and through thermal disorder), which will decrease the spin density. This will decrease the spin polarization of the potential, which in turn will decrease the spin density even more, and at some temperature T^* the support of the pseudogap from the spin wave will collapse [10]. The fact that V_q is the largest at low doping favors larger T^* when $h \to 0$. A high DOS at E_F is important for a high superconducting T_C and therefore is the pseudogap in competition with superconductivity in underdoped cuprates [13].

It was suggested that nonadiabatic electron-phonon coupling could be enhanced in the cuprates, because of the low Fermi velocity in the z-direction [25, 26]. This velocity is comparable to the vibrational velocity and the electronic screening appeared to be insufficient. However, the screening can be made by other electrons moving within the planes. Moreover, phonon frequencies calculated within LDA without assumptions of incomplete screening, agree satisfactory with experimental frequencies [19–21]. Instead, excitations of virtual phonons coupled to spin waves can be important for the mechanism of superconductivity, but SPC makes the separation between pure electron-phonon coupling, λ_{ep}, and λ caused by spin fluctuations, λ_{sf}, less clear.

The important observation is that atomic phonon distortions will trigger enhancement of spin waves. If so, the possibility for larger λ_{ep} is open, because instead for the common approach to ignore spin effects in electron-phonon coupling, there are larger matrix elements when the spin polarized part of the potential is involved. This is readily imagined for a system which is nonmagnetic when phonon distortions are absent, but magnetic when the distortions are present. An estimation of pure λ_{ep} and the coupling parameter for SPC, λ_{SPC}, in LBCO has been presented earlier [23]. With a total $N(E_F) \approx 0.9\ (\text{eV} \cdot \text{cell} \cdot \text{spin})^{-1}$, and distortion amplitudes and potential shifts as in [13] this leads to λ_s' of the order 0.36 and 0.6 for pure phonons and SPC, respectively [23]. These values appear sufficiently large for a large T_C in simple BCS-type formulations, but the precise relation for T_C depends also on other parameters [27].

The third mechanism is that spin fluctuations work without coupling to phonon excitations. Still, phonon distortions might be present and will in that case be important for enhancements of rapid (high energy) spin fluctuations. For instance, it was found that the local exchange enhancement (for AFM) on Cu sites is the largest when the surrounding atoms (La or oxygen) have been pushed away from the Cu, and this leads to SPC between phonons and spin waves with equal $\vec{q}$ and ω [13]. But strong high-ω spin excitations should also be possible on rows of Cu with

Table 1: Total energy (ΔE, mRy per Cu), matrix element for spin fluctuations (ΔV in mRy), λ_{sf}, and local Stoner enhancement, S, calculated for lattices of LBCO with two phonon distortions and without distortions.

Phonon	ΔE	ΔV	λ_{sf}	S
No phonon	12.7	9	0.03	1.6
Plane-O	8.2	12.5	0.12	2.6
La	7.4	12.0	0.11	2.4

enhanced exchange, perpendicular to the phonon. Ab initio calculations are not easy for such configurations because of the large size of the required unit cells, but one can use some of the existing results for first estimations of λ_{sf} for rapid spin fluctuation (so rapid that the phonon distortions appear to be static compared to the spin fluctuation). The enhancements depend on the different types of distortions as was discussed above. In this case we calculate $\lambda_{sf} = N\langle dV/dm\rangle^2/(d^2E/dm^2)$, where V is the potential, E is the total energy of the spin wave, and m is the magnetic moment (per Cu) [28, 29]. The difference in free energy between nonpolarized and an induced (by magnetic field) AFM wave can be written $E_m = E_0 + \kappa m^2$, so that $d^2E/dm^2 = 2\kappa$, which permits to calculate $\lambda_{sf} = N \cdot (\Delta V)^2/\kappa$ for "harmonic" spin fluctuations. With parameters from the band results this makes λ_{sf} equal to 0.03 when no lattice distortions are present, and 0.12 and 0.11 when the lattice contain distortions; see Table 1.

The frequency has not been calculated explicitly, but a shortcut via exchange enhancements can be used for a simple estimation, as for FM fluctuations [28–30]. Thus, $\omega_{sf} \approx 1/(4NS)$, where $S = \Delta V/\Delta H$ is the local Stoner enhancement (on Cu) and ΔH is the external field (5 mRy in these calculations). This makes ω_{sf} 100–200 meV depending on the type of lattice distortion. Figure 5 shows the combined results for direct λ_{SPC} and indirect λ_{sf} as function of frequency. The general shape is similar as the electron-boson coupling function that has been extracted from recent optical spectra on Hg- and Bi-based copper oxides [31].

The amplitudes of λ_{SPC} and λ_{sf} increase further if both of the latter distortions (plane oxygen *and* La) are considered in the calculation. The matrix element increases to about 14.5 mRy. Despite this relative increase, it is seen that pure spin fluctuations give not as large λ's as for SPC. This is especially clear when all lattice modes are considered. However, these pure spin fluctuations can be important for superconductivity, since they appear at large ω. In contrast, SPC is essentially limited to below the highest phonon frequency, that is, to 50–70 meV. The relatively small absolute values of λ_{sf} are partly caused by the use of LDA. Improved DF schemes, which could predict an AFM insulating state for the undoped systems, would lead to larger exchange enhancements, larger λ_{sf}, and lower ω_{sf} in doped systems.

5. Correlation and Corrections to LDA

The question is whether the real electron-electron correlation in the oxides is much larger than what is included

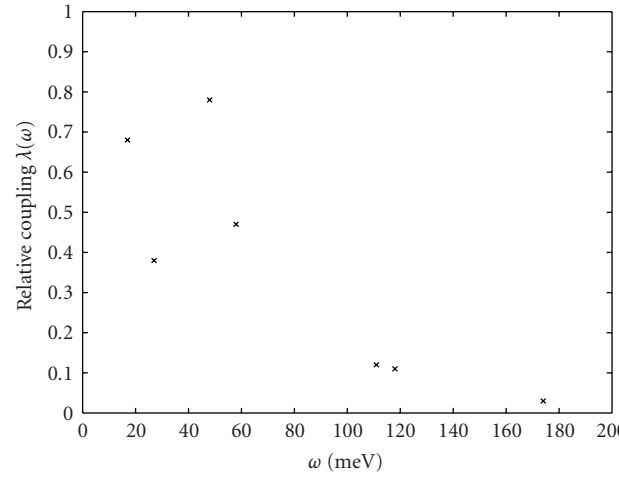

Figure 5: The relative strength of λ_{SPC} (the first 4 points) and λ_{sf} (the 3 points at the highest energies). The latter will move towards lower energy if the exchange enhancement increases, while the points for SPC are fixed near the phonon energies; see the text.

in LDA. The latter includes exchange and correlation (XC) for an electron gas of varying density with the electron gas radius $r_s = 0.62\rho^{-1/3}$ as parameter. The density ρ contains one electron within r_s. The largest values of r_s (≈ 2 a.u.) are found in the low-density valence-electron region between the atoms, but they are still smaller than any typical atomic radius, R_A in transition metals, their oxides, and these cuprates. This gives a major argument against using a strong on-site correlation parameter to an atom, because the effect of an additional electron will readily be screened out and is not noticed beyond r_s. In low-density materials, however, such as the alkali metals, $r_s \approx R_A$ and on-site correlation could be advocated. But LDA seems to describe alkali metals well, which provides an additional argument in favor of local approximations of DFT.

The fact is that LSDA does not produce an AFM insulating ground state of several oxides, and so the problem is real and it may be related to the spin-polarized part of the potential. Small errors with important consequences of this type are known for LSDA. A well-known example is for Fe, where LSDA predicts nonmagnetic (NM) face-centered cubic (fcc) lattice as the ground state, whereas the generalized gradient approximation (GGA, [6]) correctly finds the ferro magnetic (FM) body-centered cubic (bcc) ground state [32–34]. The difference between LDA and GGA is not large concerning the bands, magnetic moments, and other properties. The band properties of bcc Fe are quite good in calculations using both these DFT functionals. But the order of the total energies for FM-bcc and NM-fcc is reversed in the two cases.

An additional indication that the AFM insulating state of the cuprates is not far away in LSDA is the fact that the AFM moment depends on the number of k-points. A sufficient number of k-points is required for convergence, but early works noticed that the AFM ground state became stable if a coarse k-point mesh was used [35–37]. A similar

conclusion for the appearance of weak ferromagnetism in highly doped LBCO can be understood from DOS effects and the Stoner criterion [38]. Thus, as for Fe, a small detail can have large consequences. It might be that the total energy difference between two very different ground states (fcc nonmagnetic and bcc-magnetic for Fe, and NM metallic and AFM insulating for cuprates) are very close, so that small errors in the computational details lead to the "wrong" ground state.

Another indication of a nearby AFM state is that LMTO calculations with off-center linearization energies can stabilize AFM in $HgBa_2CuO_4$ in calculations with sufficient number of k-points. The normal procedure in LMTO is to chose linearization energies at the center of the occupied subbands, but if they are chosen at the bottom of the bands, it leads to a slight localization of the states. An AFM order needs less hybridization energy and AFM can be stabilized [39]. This is rather ad hoc, since LMTO should not be made in such a way. A theoretical justification is need for a better DFT scheme.

A first workable nonlocal density functional is the GGA (generalized gradient correction [6]), where the gradient, or the first derivative of the charge density, $d\rho(r)/dr$, brings out corrections to the LSDA. The gradients are mainly radial in atoms and solids because of the steep drop in charge density for increasing r close to an atom. Only valence electrons have large amplitudes in the interstitial region between the atoms, where the gradients are moderate. However, higher gradients such as the second derivative of the density can be large in the interstitial, a feature not captured by the GGA. Nevertheless, by using GGA in the LMTO calculations for LBCO there is some improvement, since the required critical magnetic field for having a gap is reduced by about 25 percent compared to LSDA.

Densities with quadratic dependence as function of r around a fixed point at $r = 0$ are used in a 2-particle model for calculations of correlation including corrections due to the second derivatives. A noninteracting density with quadratic gradients has the form

$$\rho(r) = \rho_0 + \frac{d^2\rho}{dr^2}\frac{r^2}{2}. \tag{1}$$

The Schrödinger equation is solved for a density of electrons surrounding a fixed electron at $r = 0$, where it is taken into account that the effective mass is 1/2 [40, 41]. The interacting potential can be written as

$$V(r) = \frac{e^2}{r} + \frac{\ell(\ell+1)}{r^2} + \mu_{\mathrm{xc}}(r) + V_{\mathrm{ext}}(r). \tag{2}$$

The exchange correlation within the surrounding electron cloud is taken into account through LDA (μ_{xc}), and the external potential V_{ext} can include relative kinetic energy variations. The two last terms in $V(r)$ are not very important for the results for gradient variations. The strongest term is the unscreened Coulomb repulsion that diverges at $r = 0$. The second term, the centrifugal term, is included only for exchange (with $\ell = 1$, higher ℓ will have higher energy), when the Pauli principle requires that the density for equal spin must be zero at $r = 0$ [41].

The solution $\Psi(E, r)$ of the Schrödinger equation for this potential is used to calculate the XC energy as the difference in Coulomb energy between interacting and noninteacting densities; $\mu = \int(\Psi(E,r)^2 - \rho(r))/r d^3r$. The energy E is determined from a required boundary condition of $\Psi(E, r_s)$. The variation of the correlation potential on the second gradient is quite easy to understand. If the gradient is positive, so that there is a tendency for a "hole" at $r = 0$, it will be less effective for the Coulomb repulsion to make the correlation hole deeper at this point. Therefore, μ_c will decrease for positive density gradients near the interstitial region. The gradient can change closer to the high-density regions near the nuclei and make the correlation larger than for a constant density, but correlation becomes negligible in comparison to exchange when the density is high. The C-correction is parametrized through the electron gas parameter r_s and $Q = \rho(r_s)/\rho(0)$, so that $C = 1 - 5\sqrt{Q}/4 + \sqrt{(r_s)} * Q/2$ for $Q > 1$ and as the inverse of this parametrization if $Q < 1$. The expression is only applied for Q between -0.25 and 0.8, and $C - 1$ is used as a scaling factor of the correlation part from LDA. This correction makes the potential a little more repulsive in the interstitial region. The Cu-d states become more localized, which can promote AFM order; see Table 2.

One fundamental theorem of DFT is that of "v-representability", that essentially says that there is a one-to-one correspondence between the density $\rho(r)$ and potential $V(r)$ [4]. The only possibility is that two equivalent charge densities can give an uninteresting shift in the potential, which can be absorbed by the shift of the energy spectrum. Imagine now that an external potential is applied to an electron gas of varying density $\rho(r)$. The free electron wave functions will oscillate more if more kinetic energy is given to the electron gas, or less if kinetic energy is subtracted, even if ρ remains constant. The exchange part of the potential (X) will be modified because of the ability of the wave function to readjust itself around a second electron of the same spin (to create an exchange "hole"), as can be imagined from Slater exchange [7] or the two-particle model [41]. A similar change occurs for correlation (C), which is caused by the immediate Coulomb repulsion between all electron pairs. If ρ is constant in space, there is only an uninteresting potential shift, but for varying charge densities there can be more subtle effects. The LDA is derived from the principle of density variations at the Fermi energy, and the relation between E_F (which is a measure of the kinetic energy) and density is given by

$$E_F^{(1)}(r) = \left(3\pi^2\rho(r)\right)^{2/3}. \tag{3}$$

This relation can be compared to $E_F^{(2)}(r) = E_F - V(r)$ within real atoms, where E_F is from the band calculation with potential $V(r)$. Except for r very close to the nuclei there is not too large difference between $E_F^{(1)}(r)$ and $E_F^{(2)}(r)$. In some regions the two values can be quite different. If so, it implies that the density is not in equilibrium with the kinetic energy as was used in the derivation of the LDA potential. Oxygen sites in oxides are often negatively charged, which suggests that the kinetic energy should be smaller than what comes out from (1). These effects are moderated by the fact that the

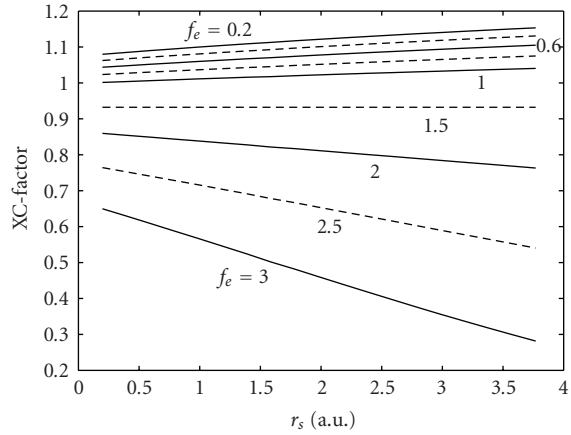

Figure 6: The calculated values of the scaling function X as function of r_s and f_e (see text).

Table 2: The required applied magnetic fields (in mRy on Cu) in order to obtain a zero gap in LMTO calculations which include the different corrections to the potential; see the text.

LSDA	GGA	GGA+C	GGA+X	GGA+C+X
8.8	6.6	5.5	5.0	4.0

charge transfer is a result of an attractive potential. It turns out that positive and negative deviations from (1) exist in shells within all atoms.

Thus, band calculations with correction for the kinetic energy will be attempted where the local exchange potential is written as

$$\mu_x(f_e, r_s) = X(f_e, r_s)\mu_{KS}(r_s), \tag{4}$$

where $X(f_e, r_s)$ is a scaling function of the normal Kohn-Sham potential μ_{KS}, and $f_e = E_F^{(1)}(r_s)/E_F^{(2)}(r_s)$.

A derivation of the scaling function $X(f_e, r_s)$ can be done directly from the Slater functions by use of energy shifts in the arguments of the plane waves [7]. However, negative shifts leading to localized waves have to be avoided, and the resulting X-function seems too sensitive to small variations of f_e. As an alternative we determine the scaling function from a two-particle model as in [40, 41], with a renormalization to make $X(1, r_s) = 1$. The result is displayed in Figure 6 for the appropriate range of r_s and f_e. The real value of f_e for $r \leq 0.05\, R_{\mathrm{RWS}}$ increases and can be larger than 50 near the nuclei. This is extreme and f_e is here cut-off at 3.

In preliminary calculations for undoped LBCO we do a rescaling of the exchange due to kinetic energy and of correlation due to second gradients. The comparison is made with standard LSDA for an AFM unit cell where a staggered magnetic field is applied to the Cu sites, and it is found that a field of $\pm$ 8.8 mRy is the limit for having a zero gap ($E_g \sim 0.25$ mRy). The magnetic moment is then $\pm 0.18\, \mu_B$ per Cu. The amplitude of the required magnetic field to obtain a zero gap is reduced when the calculations include the correction factors; see Table 2. The absolute values can depend on details of the band calculations [39], but the trend towards a stability of an AFM state is clear. Corrections of this type will be interesting for seeing enhanced spin fluctuations for long wave length spin waves in doped cuprates. Further enhancements of λ_{sf} can also be expected [13]. Potential corrections must ultimately be tested for other types of materials in order to verify that some properties will not deteriorate. Here for the cuprates the corrections permit to proceed in the modeling of more properties from the band results.

6. Conclusion

Results of band calculations for supercells with frozen phonons and spin waves suggest that a Fermi-liquid state can cause pseudogaps and dynamic stripes. Together with an NFE model it is possible to describe the doping dependence of many normal state properties of the cuprates. The coupling between phonon distortions and spin fluctuations seems to be crucial for the mechanism of superconductivity, so that the spin-polarized part of λ is most enhanced by simultaneous excitations of phonons and spin waves. Two different mechanisms for superconductivity mediated by spin fluctuations are possible. The largest coupling parameter is when a phonon is excited together with the spin fluctuation. Lower couplings, λ_{sf} at larger energies, are independent of the phonon excitation, but these spin fluctuations can nevertheless profit from possible phonon distortions of the lattice. Still, absolute numbers are too small when using LDA, as is also concluded from the absence of AFM stability in LDA calculations for undoped systems. However, it is argued that corrections due to higher-order density gradients and kinetic energy are able to bring the band calculations closer to AFM. This is shown in calculations for undoped LBCO by yet very approximate corrections due to nonlocality and kinetic energy. Refinements of such corrections will be of interest for application to supercells, including doping, phonon distortions, and spin waves, since it can be expected that realistic λ_s' will be obtained.

References

[1] J. Orenstein and A. J. Millis, "Advances in the physics of high-temperature superconductivity," *Science*, vol. 288, no. 5465, pp. 468–474, 2000.

[2] M. T. Czyżyk and G. A. Sawatzky, "Local-density functional and on-site correlations: the electronic structure of La_2CuO_4 and $LaCuO_3$," *Physical Review B*, vol. 49, no. 20, pp. 14211–14228, 1994.

[3] A. Damascelli, Z.-X. Shen, and Z. Hussain, "Angle-resolved photoemission studies of the cuprate superconductors," *Reviews of Modern Physics*, vol. 75, no. 2, pp. 473–541, 2003.

[4] W. Kohn and L. J. Sham, "Self-consistent equations including exchange and correlation effects," *Physical Review*, vol. 140, no. 4A, pp. A1133–A1138, 1965.

[5] O. Gunnarsson and B. I. Lundqvist, "Exchange and correlation in atoms, molecules, and solids by the spin-density-functional formalism," *Physical Review B*, vol. 13, no. 10, pp. 4274–4298, 1976.

[6] J. P. Perdew and W. Yue, "Accurate and simple density functional for the electronic exchange energy: generalized

gradient approximation," *Physical Review B*, vol. 33, no. 12, pp. 8800–8802, 1986.

[7] J. C. Slater, "A simplification of the Hartree-Fock method," *Physical Review*, vol. 81, no. 3, pp. 385–390, 1951.

[8] T. Jarlborg, "Spin waves and large electron-phonon coupling near the metal-insulator transition in hole-doped high-T_c oxides," *Physical Review B*, vol. 64, no. 6, Article ID 060507, 4 pages, 2001.

[9] T. Jarlborg, "Spin-phonon interaction and band effects in the high-T_c superconductor $HgBa_2CuO_4$," *Physical Review B*, vol. 68, no. 17, Article ID 172501, 4 pages, 2003.

[10] T. Jarlborg, "Effects of spin-phonon interaction within the CuO plane of high-T_C superconductors," *Physica C*, vol. 454, no. 1-2, pp. 5–14, 2007.

[11] O. K. Andersen, "Linear methods in band theory," *Physical Review B*, vol. 12, no. 8, pp. 3060–3083, 1975.

[12] T. Jarlborg and G. Arbman, "The electronic structure of some A15 compounds by semiself-consistent band calculations," *Journal of Physics F*, vol. 7, no. 9, pp. 1635–1649, 1977.

[13] T. Jarlborg, "Properties of high-T_C copper oxides from the nearly-free-electron model," *Physical Review B*, vol. 76, no. 14, Article ID 140504, 4 pages, 2007.

[14] T. Jarlborg, "Spin-phonon interaction in doped high-T_C superconductors from density functional calculations," *Physics Letters A*, vol. 295, no. 2-3, pp. 154–159, 2002.

[15] T. Jarlborg, "Properties of high-T_C copper oxides from band models of spin-phonon coupling," *Journal of Superconductivity and Novel Magnetism*, vol. 22, no. 3, pp. 247–250, 2009.

[16] T. Jarlborg, "Mechanisms for higher T_C in copper oxide superconductors: ideas from band calculations," *Applied Physics Letters*, vol. 94, no. 21, Article ID 212503, 2009.

[17] J. Humlíček, A. P. Litvinchuk, W. Kress, et al., "Lattice vibrations of $Y_{1-X}Pr_XBa_2Cu_3O_7$: theory and experiment," *Physica C*, vol. 206, no. 3-4, pp. 345–359, 1993.

[18] C. Thomsen and M. Cardona, "Raman scattering in high-T_c superconductors," in *Physical Properties of High-Temperature Superconductors*, D. M. Ginsberg, Ed., vol. 409, World Scientific, Singapore, 1989.

[19] H. Chen and J. Callaway, "Phonons and superconductivity in $Nd_{2-x}Ce_xCuO_4$," *Physical Review B*, vol. 46, no. 21, pp. 14321–14324, 1992.

[20] R. E. Cohen, W. E. Pickett, and H. Krakauer, "Theoretical determination of strong electron-phonon coupling in $YBa_2Cu_3O_7$," *Physical Review Letters*, vol. 64, no. 21, pp. 2575–2578, 1990.

[21] O. K. Andersen, A. I. Liechtenstein, O. Rodriguez, et al., "Electrons, phonons, and their interaction in $YBa_2Cu_3O_7$," *Physica C*, vol. 185–189, pp. 147–155, 1991.

[22] T. Jarlborg and G. Santi, "Role of thermal disorder on the electronic structure in high-T_c compounds," *Physica C*, vol. 329, no. 4, pp. 243–257, 2000.

[23] T. Jarlborg, "Spin-phonon coupling and q -dependence of spin excitations and high-T_c superconductivity from band models," *Physical Review B*, vol. 79, no. 9, Article ID 094530, 7 pages, 2009.

[24] P. Piekarz and T. Egami, "Dynamic charge transfer and spin-phonon interaction in high-T_c supeconductors," *Physical Review B*, vol. 72, no. 5, Article ID 054530, 9 pages, 2005.

[25] T. Jarlborg, "Weak screening of high frequency phonons and superconductivity in $YBa_2Cu_3O_7$," *Solid State Communications*, vol. 71, no. 8, pp. 669–671, 1989.

[26] T. Jarlborg, "Restricted screening and non-adiabatic electron-phonon coupling in high-T_c oxides," *Physics Letters A*, vol. 164, no. 3-4, pp. 345–348, 1992.

[27] A. Abanov, A. V. Chubukov, and M. R. Norman, "Gap anisotropy and universal pairing scale in a spin-fluctuation model of cuprate superconductors," *Physical Review B*, vol. 78, Article ID 220507, 4 pages, 2008.

[28] T. Jarlborg, "Spin fluctuations, electron-phonon coupling and superconductivity in near-magnetic elementary metals—Fe, Co, Ni and Pd," *Physica C*, vol. 385, no. 4, pp. 513–524, 2003.

[29] T. Jarlborg, "Ferromagnetic and antiferromagnetic spin fluctuations and superconductivity in the hcp-phase of Fe," *Physics Letters A*, vol. 300, no. 4-5, pp. 518–523, 2002.

[30] I. I. Mazin and D. J. Singh, "Ferromagnetic spin fluctuation induced superconductivity in Sr_2RuO_4," *Physical Review Letters*, vol. 79, no. 4, pp. 733–736, 1997.

[31] E. van Heumen, E. Muhlethaler, A. B. Kuzmenko, et al., "Optical determination of the relation between the electron-boson coupling function and the critical temperature in high-T_c cuprates," *Physical Review B*, vol. 79, no. 18, Article ID 184512, 7 pages, 2009.

[32] J. Kübler, "Magnetic-moments of ferromagnetic and antiferromagnetic bcc and fcc iron," *Physics Letters A*, vol. 81, p. 81, 1981.

[33] C. S. Wang, B. M. Klein, and H. Krakauer, "Theory of magnetic and structural ordering in iron," *Physical Review Letters*, vol. 54, no. 16, pp. 1852–1855, 1985.

[34] B. Barbiellini, E. G. Moroni, and T. Jarlborg, "Effects of gradient corrections on electronic structure in metals," *Journal of Physics: Condensed Matter*, vol. 2, no. 37, pp. 7597–7611, 1990.

[35] T. C. Leung, X. W. Wang, and B. N. Harmon, "Band theoretical study of magnetism in Sc_2CuO_4," *Physical Review B*, vol. 37, pp. 384–388, 1988.

[36] G. Y. Guo, W. M. Temmermann, and G. M. Stocks, "On the metal-semiconductor transition and antiferromagnetism in La_2CuO_4," *Journal of Physics C*, vol. 21, p. L103, 1988.

[37] W. E. Pickett, "Electronic structure of the high-temperature oxide superconductors," *Reviews of Modern Physics*, vol. 61, no. 2, pp. 433–512, 1989.

[38] B. Barbiellini and T. Jarlborg, "Importance of local band effects for ferromagnetism in hole-doped La_2CuO_4 cuprate superconductors," *Physical Review Letters*, vol. 101, no. 15, Article ID 157002, 2008.

[39] T. Jarlborg, "Anti-ferromagnetism, spin-phonon interaction and the local-density approximation in high-T_C superconductors," *Journal of Physics: Condensed Matter*, vol. 16, no. 13, pp. L173–L178, 2004.

[40] B. Barbiellini and T. Jarlborg, "A simple approach towards non-local potentials: theory and applications," *Journal of Physics: Condensed Matter*, vol. 1, no. 45, pp. 8865–8876, 1989.

[41] T. Jarlborg, "Pair correlation functions for exchange and correlation in uniform spin densities," *Physics Letters A*, vol. 260, no. 5, pp. 395–399, 1999.